Ann. For. Res. 64(2): 203-210, 2021
ISSN: 18448135, 20652445

ANNALS OF FOREST RESEARCH
www.e-afr.com

DETECTION OF DEFORESTATION CHANGE IN SAR IMAGES USING LOCAL FEATURES

Gayatri Mirajkar
Arvind Gavali College of Engineering, Satara, Maharashtra, India
gayatrimirajkar@gmail.com

Abstract
To recognize deforestation utilizing Earth Observation (EO) information, generally utilized techniques depend on the identification of fleeting changes in the EO estimations inside the deforested patches. In this paper, we present another mark of deforestation got from manufactured gap radar (SAR) pictures, which depends on a mathematical curio that seems when deforestation occurs, as a shadow at the boundary of the deforested area. The circumstances for the presence of these shadows are investigated, too as the strategies that can be utilized to take advantage of them to distinguish deforestation. The methodology includes two stages: (1) location of new shadows; (2) remaking of the deforested fix around the shadows. The data from Sentinel-1 of 2014 has opened up valuable open doors for a likely application of this methodology in huge scope applications. A deforestation identification technique in view of this approach was tried in a 600,000 ha site in Peru. A recognition accuracy of over 95% is gotten for tests bigger than 0.4 ha, and the strategy was found to perform better compared to the optical-based UMD-GLAD Alerts GLAD Forest Alert dataset both with regards to spatial and transient identification. Further work expected to take advantage of this methodology at functional levels is also considered.
Key: Detection. Deforestation, Change, SAR Images, Local Features.

Introduction
[7] To perceive deforestation using Earth Observation (EO) data, for the most part used procedures rely upon the recognizable proof of passing changes in the EO assessments inside the deforested patches. In this paper, we present one more sign of deforestation got from synthetic aperture radar (SAR) pictures, which relies upon a numerical artifact that appears when deforestation happens, as a shadow at the limit of the deforested patch [7],[8], [9] The conditions for the presence of these shadows are explored, too as the methodologies that can be used to exploit them to recognize deforestation.[9][12][14] The technique incorporates two phases: (1) area of new shadows; (2) reconstruction of the deforested patch around the shadows [8], [9] The launch of Sentinel-1 in 2014 has opened up important entryways for a possible cheating of this system in colossal degree applications. A deforestation distinguishing proof strategy considering this approach was attempted in a 600,000 ha site in Peru. An detection rate of more than 95% is gotten for tests greater than 0.4 ha, and the system was found to perform better contrasted with the optical-based UMD-Cheerful Forest Caution dataset both concerning spatial and transient ID. Further work expected to exploit this procedure at practical levels is discussed.

© ICAS 2021

Satellite imagery is the essential device for giving data on recently deforested regions in immense and some of the extremely distant timberlands [5], with most verification approaches depending dominatingly on optical remote sensing. Specifically, animated by the launch of the Landsat document in combination with the capacity to download completely pre-processed pictures, endeavors lately moved towards functional and huge scope deforestation observing frameworks in light of Landsat time series, at yearly scales [6, 7] or even with close continuous (NRT) abilities [8].

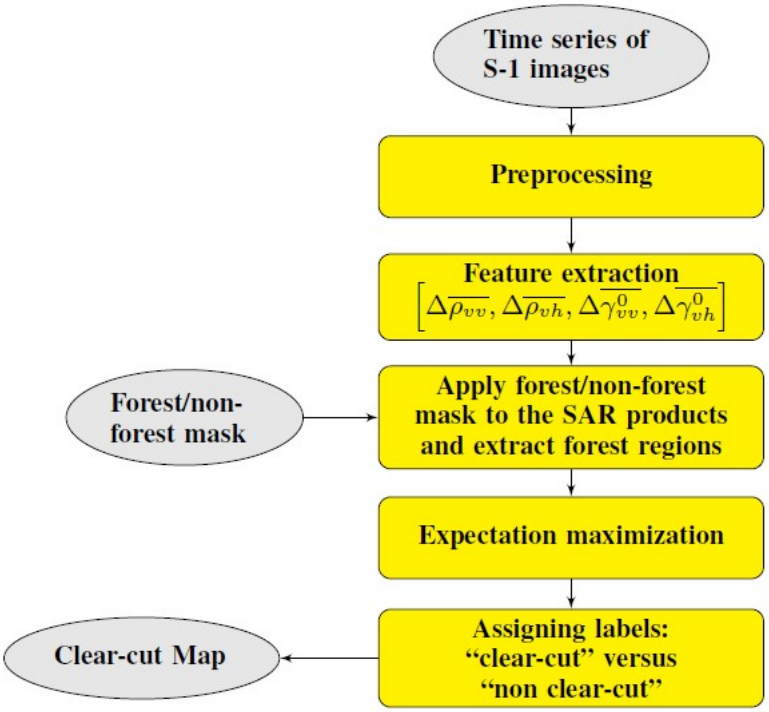

Fig.1: Detection of Deforestation Change in SAR Images Using Local Features Flow Chart

Hansen et al. (2016) [8] exhibited the potential for and requirements of functional Landsat based deforestation alerts for the tropical jungles. A significant limit for optical-based NRT applications is the presence of fog in the dry season (brought about by fire) and, all the more critically, of mists in the wet season [7, 8,9,10]. A few locales experience the ill effects of inescapable overcast cover all through the whole year, and, surprisingly, over one year [8,10,11]. Consolidating Sentinel-2 (S2) information would increment information wealth and work on the discovery of progress. Utilizing manufactured gap radar (SAR) is another choice.

Materials and Methods

The exploratory piece of this paper centers around a review site of 600,000 ha (93 km × 65 km) situated in the Peruvian Amazon,. The review site lies on the eastern side of the Andes and covers the boundary between the San Martin and Loreto areas, around the city of Yurimaguas. The site

© ICAS 2021

contains a generally safeguarded bumpy region, Cordillera Escalera, in its western part, while the eastern part has a place with the Amazon marshes. The normal vegetation includes for the most part evergreen rainforest, with the presence of some occasional deciduous woodland. In the swamps, the region is vigorously corrupted by smallholder farming (rice, papaya, vegetables) as well as late agro-modern improvement comparable to the palm oil and cocoa industry, which prompted huge deforestation occasions.

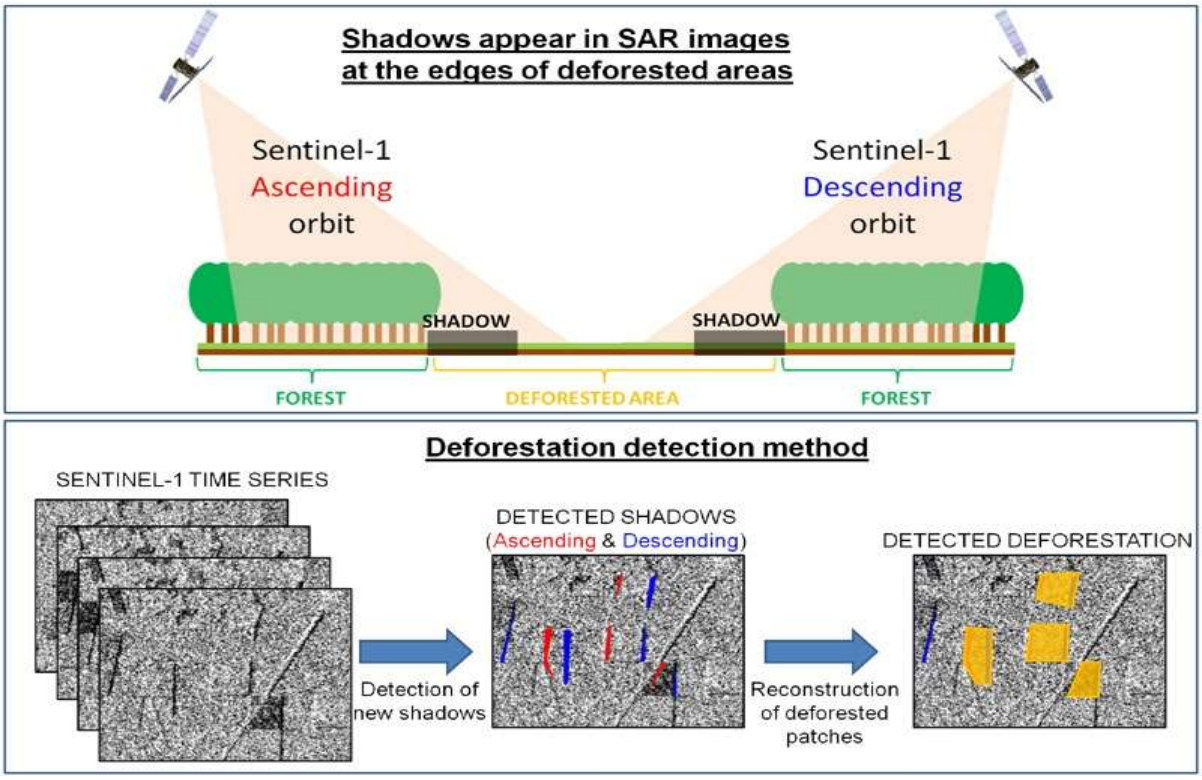

Fig.2: Detection of Deforestation Change in SAR Images Using Local Features process Reference Data

To approve the deforestation planning results, we utilized reference tests got from two Sentinel-2 pictures gained on 10 March 2016 and 16 October 2016, which are the just nearly sans cloud Sentinel-2 pictures procured in 2016. The example choice was accomplished in two stages. In the first place, we physically chose 94 deforestation tests through visual understanding of the two Sentinel-2 pictures, as well as 32 undisturbed examples.

Then, at that point, these physically chosen deforestation tests were utilized to survey the ghostly marks of deforestation occasions (NDVI, red, green, and blue groups at the two dates), and these marks were utilized to construct a choice tree that consequently separates reference tests from the Sentinel-2 pictures. A further visual quality check was finished to guarantee that the extricated tests really compared to deforestation. Altogether, 901 reference deforestation tests have been

© ICAS 2021

removed consequently, which address deforestation occasions that happened between the two Sentinel-2 acquisitions.

Methods

As referenced in the presentation, deforestation isn't generally described by a massive difference in backscatter inside the upset region. To get around this issue, we fostered an elective technique which comprises in identifying SAR shadowing. Shadowing happens in SAR pictures on account of the specific side-looking review math of SAR frameworks. A shadow in a SAR picture is a region that can't be arrived at by any radar beat, on the grounds that higher items make a hindrance between the SAR recieving wire and this region. Thus, no backscatter is recorded at these areas, and shadows address dull regions in the SAR pictures. This peculiarity regularly happens in uneven regions where high pinnacles make shadows, however shadows made by trees at the lines among woods and non-woodland regions can likewise be seen in high-goal SAR pictures, contingent upon the survey heading,.

Shadows that appear are described by an unexpected drop of backscatter in the S1 time series. On account of the absolutely mathematical nature of the shadowing impacts, this reduction of backscatter is supposed to be diligent over the long haul. New shadows ought to therefore stay noticeable for an extensive stretch. Going against the norm, as recently referenced, the reduction of backscatter that is in some cases seen inside a deforested region is for the most part not steady in that frame of observation, of natural circumstances, regrowth, or woodland the executives. Similarly, shadows that vanish are hypothetically portrayed by an unexpected increment of backscatter, however these shadows are displaced by exposed soil, with possibly low and variable backscatter, and can subsequently be trying to identify.

At the point when a patch is deforested inside a woodland, notwithstanding the shadow that shows up on one of its edges (for a given circle direction), a contrary phenomenon is some of the time observed on the contrary edge: a backscatter increment, brought about by a double-bounce mechanism between the recently created uncovered ground and the trees at the boundary of the excess woodland [26]. Notwithstanding, in light of the fact that this impact relies upon the backscatter of the uncovered ground, it is subject to the natural circumstances, and is subsequently more variable and less persevering than the shadowing impact. We in this way focused exclusively around the identification of recently made shadows, as being the most solid mark of deforestation is accepted.

Table. Confusion matrix of S1-based approach.

© ICAS 2021

		Reference		
		Disturbed	Not Disturbed	UA (%)
Detection	Disturbed	29,082	162	99.4
	Not disturbed	7155	202,491	96.6
	PA (%)	80.3	99.9	

Table. Confusion matrix of UMD-GLAD Forest Alert dataset.

		Reference		
		Disturbed	Not Disturbed	UA (%)
Detection	Disturbed	14,559	18	99.9
	Not disturbed	21,678	202,635	90.3
	PA (%)	40.2	100	

Detection of Shadows

As a matter of some importance, to be discernible, shadows must be enormous enough comparative with the goal of S1 pictures. Over level territory, the width of the shadows W is communicated as a component of the tree level H, and the SAR rate point θ: $W = H \tan(\theta)$. The width of the for the scope of rate points of S1 (somewhere in the range of 29° and 46°) and for tree levels somewhere in the range of 0 and 40 m, with the relating number of pixels.

For instance, a shadow of 10 m (i.e., a S1 pixel) happens when trees are more prominent than 10 m at 45° and 18 m at 29° roughly. On account of non-level territory, with a neighbourhood incline α situated towards the sensor ($\alpha > 0$) or away from the sensor ($\alpha < 0$), the shadow width is increased by a variable $K = \cos(\theta)*\cos(\alpha)/\cos(\theta - \alpha)$. For moderate slants beneath 10°, this infers a decrease of the shadow width restricted to 15% for inclines situated towards the sensor, and an increment of the shadow width restricted to 22% for inclines arranged away from the sensor. These mathematical attributes confine the utilization of this technique to thick woods with high trees. As per the tree level guide of Simard et al. (2011) [27], normal tree level in the Peru site is above 35.5 m in the swamp and 32.5 m in the bumpy region, which guarantees that shadows are perceivable (more than 1.5 pixel wide) in level territory and over moderate slants.

© ICAS 2021

Ann. For. Res. 64(2): 203-210, 2021
ISSN: 18448135, 20652445

Figure 03. The Sentinel-1A and -1B observation scenario valid from February 2018.

For the situation while both rising and plunging circles are first line in Figure 4, which is the most well-known design), a proficient reproduction of the deforested patches would comprise in partner the identified shadows into matches (one in climbing and one in plummeting, happening in a given area inside a decreased time span), and in applying a limit administrator (e.g., raised envelope) around these two edges to depict the deforested fix, as represented

Results

Following the methodology depicted in Segment 2, the accessible S1 dataset was utilized to deliver a guide of all deforested regions distinguished in the year 2016, the deforestation map is assessed as far as discovery rates utilizing the 901 naturally chosen deforestation reference tests portrayed in Area 2.2.2. The recognition rates relate to the level of reference tests that are accurately recognized by a given strategy, where an example is viewed as identified when no less than 10% of its area has been viewed as deforested. It hence relates to the producer's accuracy of the "disturbance" class.

The detection rates of the S1-based technique described in this paper are given (red line) for various example size ranges: 0-0.2 ha, 0.2-0.4 ha, 0.4-0.6 ha, 0.6-0.8 ha, 0.8-1 ha, 1-1.5 ha, 1.5-2 ha, 2-3 ha, 3-4 ha, 4-5 ha. A similar discovery rates were likewise determined for the UMD-GLAD Forest Alerts dataset (blue line). The quantity of reference tests in each size range is likewise announced (dark line). For the S1-just methodology, we considered just detections occurring successfully between the dates of the two Sentinel-2 pictures utilized for the example extractions (10 March to 16 October 2016), while for the UMD-GLAD dataset, we thought about every one of the

© ICAS 2021

discoveries happening in 2016, in view of the lower perception rate connected to the unfortunate accessibility of sans cloud Landsat perceptions.

However, the recognition rate is generally higher with the S1-based approach than in the UMD-GLAD Forests Alert dataset, aside from the exceptionally huge examples (north of 3 ha) where the two techniques arrive at 100 percent location (with not many examples). Specifically, the S1-based approach arrives at a 95% discovery rate as of now for tests in the reach 0.4-0.6 ha. Upsides of around 90% location rate are reached by the UMD-GLAD Forests Alert just over the 1.5-2 ha range, part of the way due to the coarser goal (30 m) of the info information.

Conclusions

In this paper, we presented another sign of backwoods aggravations that can be gotten from SAR time series, as shadow regions that show up at the edges of deforested patches. We depicted how and when these shadows show up or vanish, and how this peculiarity can be taken advantage of to identify deforestation occasions. With the send-off of S1, the accessibility of for nothing high-goal SAR information, with a worldwide inclusion and high fleeting reiteration, has permitted testing, interestingly, the capability of this methodology. We exhibited the responsiveness of the strategy in a 600,000 ha test site in the Peruvian Amazon, by getting preferable identification rates over the UMD-Happy Timberland Alert dataset, a Landsat-based NRT deforestation discovery framework, and a superior fleeting portrayal of deforestation occasions. This responsiveness will be taken advantage of in store for functional applications

References

1. Whittle, M.; Quegan, S.; Uryu, Y.; Stüewe, M.; Yulianto, K. Detection of tropical deforestation using ALOS-PALSAR: A Sumatran case study. *Remote Sens. Environ.* **2021**, *124*, 83–98.
2. Van der Werf, G.R.; Morton, D.C.; DeFries, R.S.; Olivier, J.G.J.; Kasibhatla, P.S.; Jackson, R.B.; Collatz, G.J.; Randerson, J.T. CO_2 emissions from forest loss. *Nat. Geosci.* **2019**, *2*, 737–738.
3. Keenan, R.J.; Reams, G.A.; Achard, F.; de Freitas, J.V.; Grainger, A.; Lindquist, E. Dynamics of global forest area: Results from the FAO Global Forest Resources Assessment 2015. *For. Ecol. Manag.* **2020**, *352*, 9–20.
4. Le Quéré, C.; Andrew, R.M.; Friedlingstein, P.; Sitch, S.; Pongratz, J.; Manning, A.C.; Korsbakken, J.I.; Peters, G.P.; Canadell, J.G.; Jackson, R.B.; et al. Global Carbon Budget 2017. *Earth Syst. Sci. Data* **2018**, *10*, 405–448. [
5. Achard, F.; Stibig, H.-J.; Eva, H.D.; Lindquist, E.J.; Bouvet, A.; Arino, O.; Mayaux, P. Estimating tropical deforestation from Earth observation data. *Carbon Manag.* **2010**, *1*, 271–287.

© ICAS 2021

6. Hansen, M.C.; Potapov, P.V.; Moore, R.; Hancher, M.; Turubanova, S.A.; Tyukavina, A.; Thau, D.; Stehman, S.V.; Goetz, S.J.; Loveland, T.R.; et al. High-Resolution Global Maps of 21st-Century Forest Cover Change. *Science* **2013**, *342*, 850–853.
7. Souza, J.; Siqueira, J.V.; Sales, M.H.; Fonseca, A.V.; Ribeiro, J.G.; Numata, I.; Cochrane, M.A.; Barber, C.P.; Roberts, D.A.; Barlow, J. Ten-Year Landsat Classification of Deforestation and Forest Degradation in the Brazilian Amazon. *Remote Sens.* **2013**, *5*, 5493–5513.
8. Hansen, M.C.; Krylov, A.; Tyukavina, A.; Potapov, P.V.; Turubanova, S.; Zutta, B.; Ifo, S.; Margono, B.; Stolle, F.; Moore, R. Humid tropical forest disturbance alerts using Landsat data. *Environ. Res. Lett.* **2016**, *11*, 034008.
9. H. Yu, J. Guo, W. Huang, L. Fang, and J. Zhao, "A deep learning approach for deforestation detection using SAR data," Remote Sensing, vol. 13, no. 3, p. 530, 2021.
10. S. Li, Y. Li, Z. Jiang, C. Li, and Y. Song, "A deep learning-based method for deforestation detection using Sentinel-1 SAR data," Remote Sensing, vol. 13, no. 8, p. 1482, 2021.
11. D. Tuia, C. Persello, and L. Bruzzone, "Multitemporal SAR image classification using deep learning: A land cover change detection application," IEEE Transactions on Geoscience and Remote Sensing, vol. 55, no. 3, pp. 1329-1345, 2017.
12. P. Chen, Y. Liu, W. Wang, H. Guo, Y. Zhang, and Y. Zhang, "Detection of deforestation in tropical forests using convolutional neural networks," Remote Sensing, vol. 11, no. 22, p. 2666, 2019.
13. Y. Liu, P. Chen, W. Wang, H. Guo, Y. Zhang, and Y. Zhang, "Deep convolutional neural networks for detecting deforestation in tropical forests using multi-source remote sensing data," Remote Sensing, vol. 11, no. 16, p. 1906, 2019.
14. T. Gindele, B. Waske, and M. Franke, "Deep learning for land cover classification and object-based deforestation detection using dual-polarimetric SAR data," Remote Sensing, vol. 11, no. 17, p. 2039, 2019.
15. X. Geng, H. Wang, L. Sun, Y. Li, and Y. Li, "Deep learning-based method for detecting deforestation using multispectral remote sensing images," International Journal of Remote Sensing, vol. 42, no. 1, pp. 294-308, 2021.
16. C. Huang, W. Wei, H. Xie, Y. He, L. Sun, and J. Zhang, "A deep learning-based method for deforestation detection in the Amazon rainforest using Landsat imagery," Remote Sensing, vol. 13, no. 5, p. 860, 2021.
17. W. Wei, H. Xie, C. Huang, Y. He, L. Sun, and J. Zhang, "Monitoring deforestation in the Amazon rainforest using deep learning and Landsat imagery," International Journal of Applied Earth Observation and Geoinformation, vol. 102, p. 102274, 2021.
18. M. H. Khan, S. S. Sultana, M. S. Rahman, and M. R. Islam, "A deep learning approach for deforestation detection using Sentinel-1 SAR data," ISPRS International Journal of Geo-Information, vol. 9, no. 7, p. 441, 2020.

© ICAS 2021